Supporting Information

Quantum Dot Surface Mediated Unprecedented Reaction of Zn^{2+} and Copper Quinolate Complex

Shilaj Roy,[a] *Satyapriya Bhandari,*[a] *and Arun Chattopadhyay*[*,a,b]

[a] Department of Chemistry and [b] Centre for Nanotechnology,

Indian Institute of Technology Guwahati,

Assam-781039, India.

[*]Email: arun@iitg.ernet.in

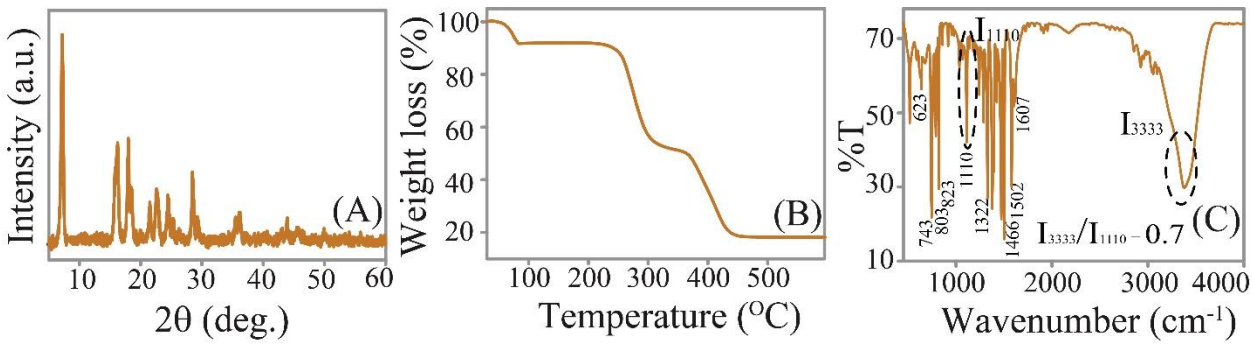

Figure S1: **(A)** Powder X-ray diffraction pattern, **(B)** thermo-gravimetric analysis (TGA) and **(C)** FTIR spectrum of solid $CuQ_2.2H_2O$ complex.[1] The presence of two strong peaks at 6.9° and 20.8° in powder XRD pattern indicated the formation of $CuQ_2.2H_2O$ complex (Figure S1A). The presence of two water molecules were confirmed through the first weight loss in TGA (Figure S1B), while the second and third weight losses in TGA curve are attributed to the partial and complete decomposition of the complex.[1-4] Importantly, the obtained ratio of 0.7 of the two bands at 3333 and 1110 cm^{-1} in FTIR spectrum also supported the octahedral nature of the complex (refer to Figure S1C). [1-3]

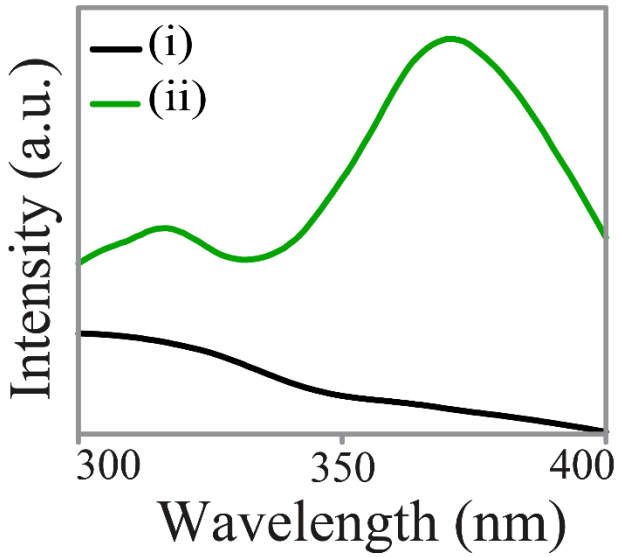

Figure S2. Excitation spectra of the ethanolic dispersion of (i) en-capped ZnS Qdots (at λ_{em}= 440 nm) and (ii) CuQ_2 added ZnS Qdots (at λ_{em}= 497 nm).

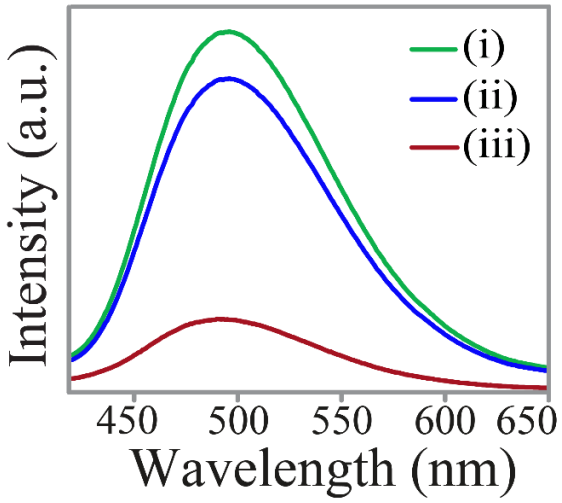

Figure S3. Emission spectra (λ_{ex}-361 nm) of CuQ_2 added *en*-capped ZnS Qdots (i) before centrifugation, (ii) of the pellet obtained after centrifugation and following redispersion into same amount of ethanol and (iii) of the supernatant after centrifugation.

Table S1. Quantum yield (%) (λ_{ex}= 361 nm) w.r.t. quinine sulphate (in 0.1 M H_2SO_4) of the ethanolic dispersion of (a) CuQ_2 added *en*-capped ZnS Qdots and (b) HQ added *en*-capped ZnS Qdots.

Samples	QY (%)
(i) CuQ_2 added *en*-capped ZnS Qdots	2.1
(ii) HQ added *en*-capped ZnS Qdots	2.9

Quantum yield calculation. The following equation was used to calculate the quantum yield of the samples, $Q_s = Q_R \times \frac{I_s}{I_R} \times \frac{A_R}{A_S} \times \frac{\eta_S^2}{\eta_R^2}$ (1)

Here, Q_S and Q_R are quantum yields of sample and reference (quinine sulphate), respectively; I_S and I_R are the areas under emission curve of sample and reference, respectively; A_S and A_R are the absorbance of the sample and reference, respectively; η_S and η_R are the refractive indices of

the solvent in which sample and reference were dissolved; Q_R is the Q.Y. of reference (here quinine sulphate) which is 0.54 (54 %). It may be noted here that absorbance of all the samples were fixed at 0.10 ± 0.01 at their individual excitation wavelength (as mentioned in the table S1).

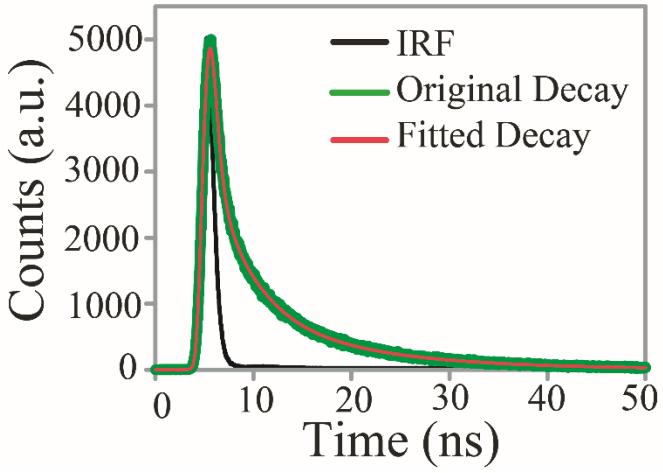

Figure S4. Photoluminescence decay profile (using 340 nm LASER) of the ethanolic dispersion of CuQ_2 added en-capped ZnS Qdots (λ_{em}=497 nm) and the graph fitted with a tri-exponential function. Here IRF stands for instrument response function.

Table S2. Decay parameters (using 340 nm LASER) obtained following by tri-exponential fitting of the emission curve of the ethanolic dispersion of CuQ_2 added en-capped ZnS Qdots (λ_{em}=497 nm).

Samples	α_i (%)	τ_i (ns)	τ_{av} (ns)	χ^2
CuQ_2 added en-capped ZnS Qdots	32.49	3.72	10.52	1.07
	19.00	0.35		
	48.51	12.04		

Life time calculation. The decay profile was fitted to a multi-exponential model using following equation

$$I(t) = \sum_i \alpha_i \exp\left(-t/\tau_i\right) \qquad (2)$$

Where, single, bi and tri exponential functions were used to fit respective emission with obtaining χ^2 close to 1.0. The averaged life times (τ_{av}) in Table S2, determined from the results of three exponential model using

$$\tau_{av} = \frac{\sum_i \alpha_i \tau_i^2}{\sum_i \alpha_i \tau_i} \qquad (3)$$

Where, α_i and τ_i are the pre-exponential factors and excited-state luminescence decay time associated with the *i*-th component, respectively.

Table S3. Zeta potential values of the ethanolic dispersion of (a) en-capped ZnS Qdots and (b) CuQ_2 added en-capped ZnS Qdots.

Samples	Zeta potential (mV)
(i) en-capped ZnS Qdots	18.9 ± 0.36
(ii) CuQ_2 added en-capped ZnS Qdots	25.3 ± 0.98

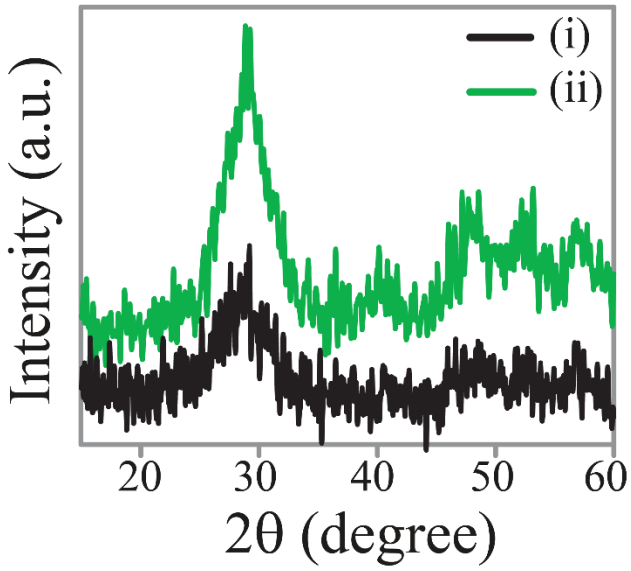

Figure S5. Powder x-ray diffraction (XRD) pattern of the solid particles of (i) en-capped ZnS Qdots and (ii) CuQ_2 added en-capped ZnS Qdots.

It has been demonstrated that the wurtzite phase of the ZnS nanocrystals are preferably formed over cubic one when ethylene diamine is used as capping ligand and the synthesis is carried out at an above 100 °C. The emergence of six peaks at 2θ = 26.2º, 28.9º, 32.7º, 40.2º, 47.6º, 52.5º and 56.9º due to (100), (002), (101), (102), (110), (103), and (112) characteristic planes clearly indicated the formation of the wurtzite phase of ZnS.[5] The morphology of the wurtzite remained unaltered following complexation/reaction with CuQ_2.

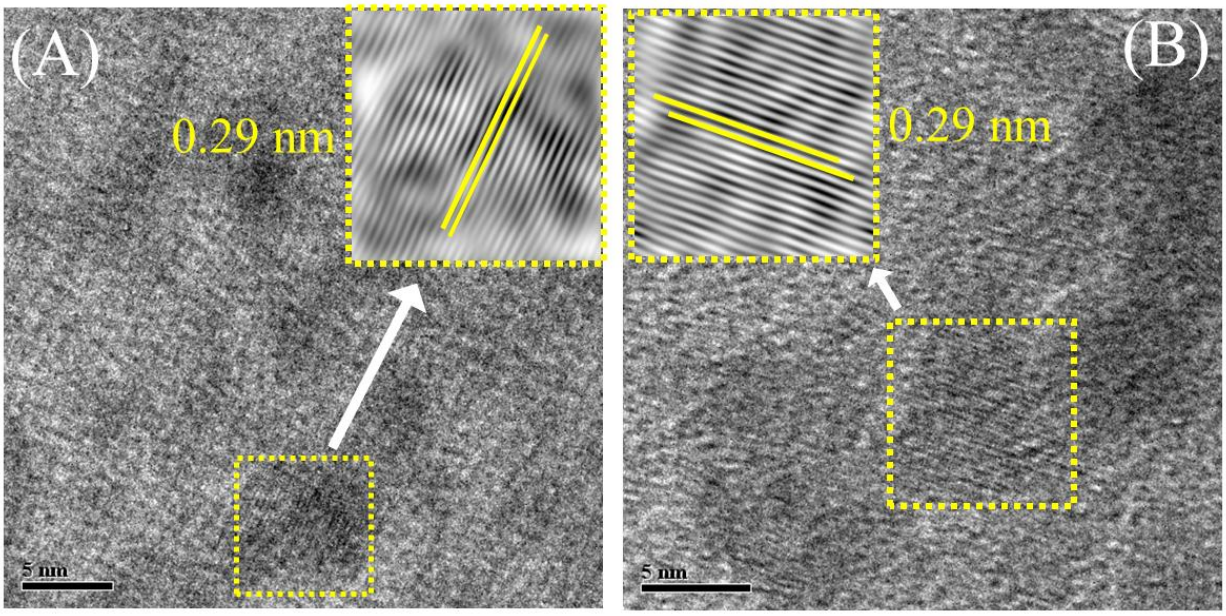

Figure S6. High resolution TEM (HRTEM) and corresponding inverse fast Fourier transform (IFFT) images of the ethanolic dispersion of **(A)** en-capped ZnS Qdots and **(B)** CuQ_2 added en-capped ZnS Qdots. The lattice spacing (0.29 nm) is due to the (002) plane of wurtzite ZnS – which was preserved following complexation/reaction with CuQ_2.[5]

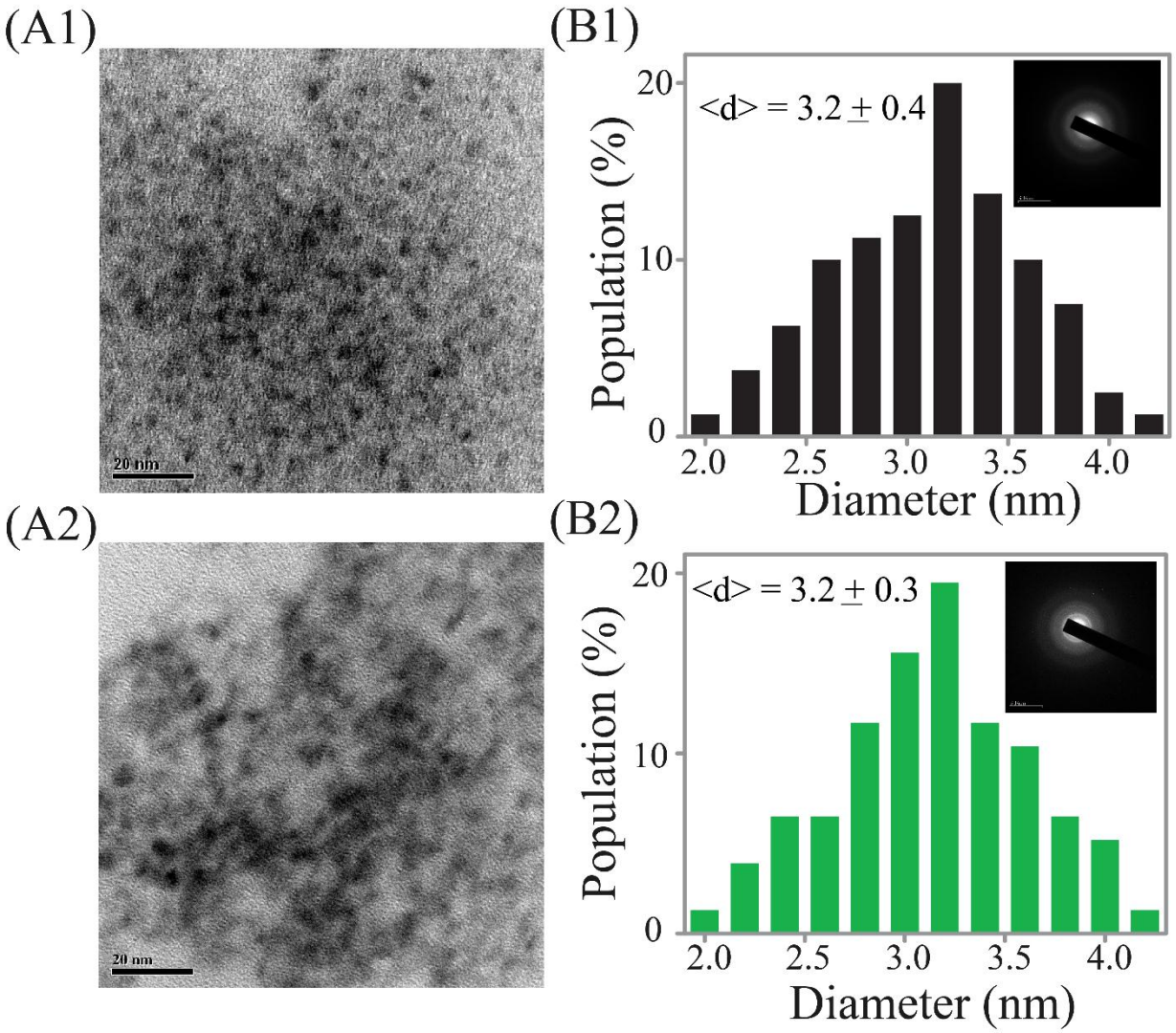

Figure S7. (A) TEM (scale bar-20 nm) image, **(B)** corresponding particle size distribution (inset: selected area diffraction pattern; scale bar 5 nm^{-1}) of the ethanolic dispersion of (1) en-capped ZnS Qdots and (2) CuQ_2 added en-capped ZnS Qdots.

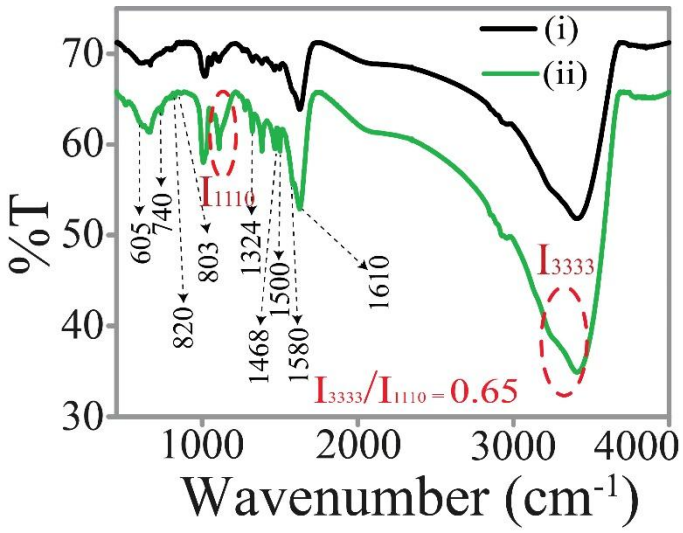

Figure S8. Fourier transform infrared (FTIR) spectra of the solid particles of (i) en-capped ZnS Qdots and (ii) CuQ_2 added en-capped ZnS Qdots. The characteristic peaks at 1605 and 1577 cm^{-1} (C-C/C-N stretching), 1500 and 1468 cm^{-1} (pyridyl and phenyl rings), at 1328 cm^{-1} (C-H bending peaks), 822, 800 and 742 cm^{1} (C-H out plane wagging) and 742, 642 and 605 cm^{-1} (in-plane ring deformation) revealed the presence metal-HQ complexes – which are absent in as synthesized Qdots – in CuQ_2 treated Qdots (SI, Figure S8i). Additionally, the presence of peak at 1110 cm^{-1} due to metal coordinated HQ in CuQ_2 treated Qdots (-C-O-M). Further, the obtained ratio of peak intensity at 3333 cm^{-1} and 1110 cm^{-1} being 0.7 indicates the octahedral nature of the surface attached MQ_2 complexes. [1-3]

Table S4: Tabulated metal ion concentration of the (i) as synthesized en-capped ZnS Qdots and (ii) CuQ_2 added en-capped ZnS Qdots (following centrifugation and redispersion into same amount of solvent). The measurements were made using an atomic absorption spectrometer.

Samples	[Zn] (ppm)	[Cu] (ppm)
(i) en-capped ZnS Qdots	46.8	-
(ii) CuQ_2 added en-capped ZnS Qdots	43.2	0.967

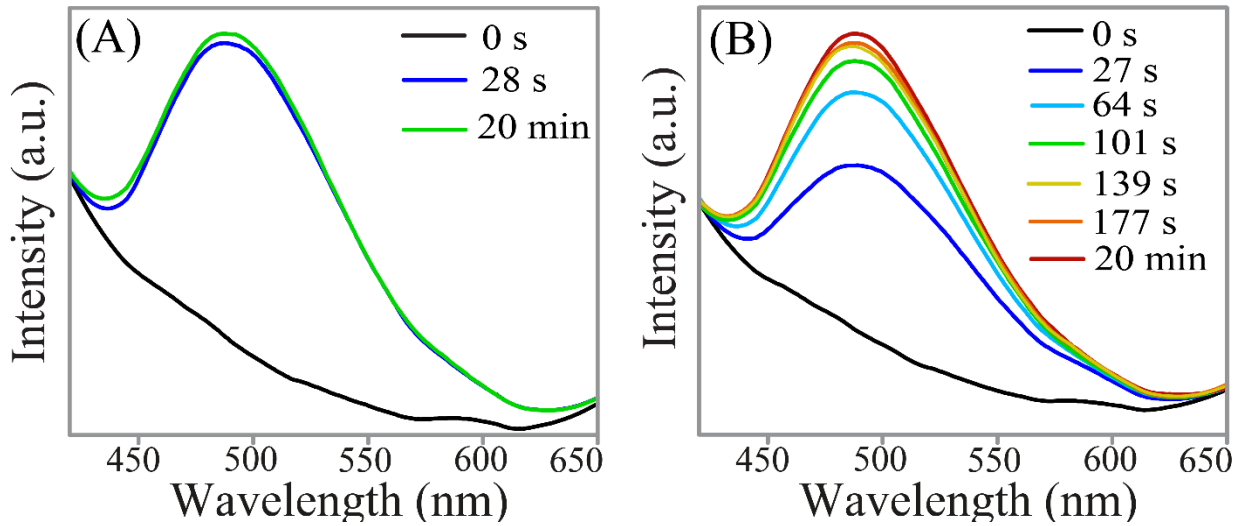

Figure S9. Time dependent changes (at T= 20 °C) in emission (λ_{ex}-361 nm) intensity following addition of **(A)** 10.0 µL 0.02 mM of HQ and **(B)** 10.0 µL 0.01 mM of MnQ_2 (in ethanol) to a solution containing 200.0 µL of as prepared Qdots (in ethanol) and 2.8 mL ethanol.

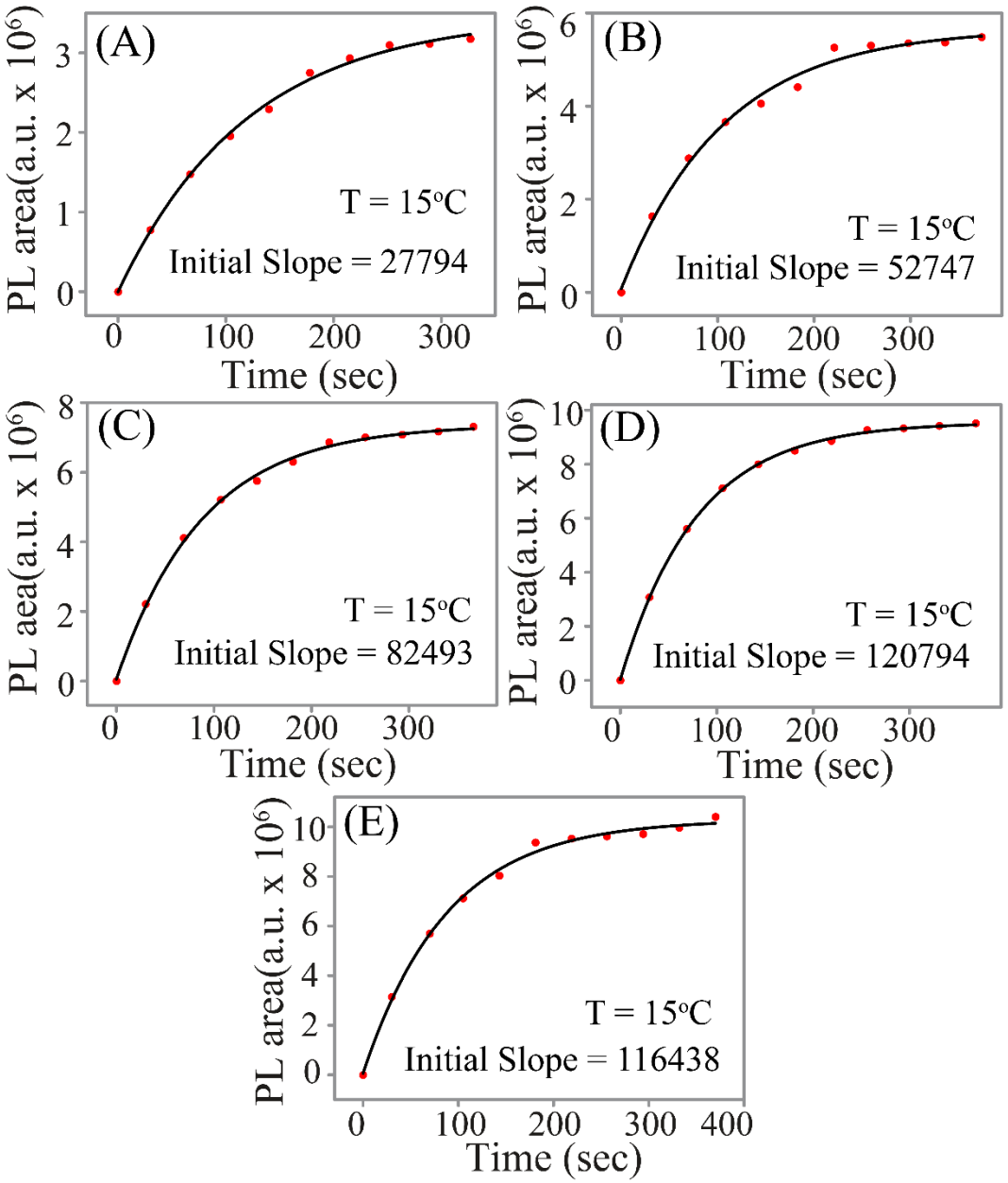

Figure S10. Exponential fittings of PL Area (area under the emission curve) vs time plot at T= 15 °C obtained from time-dependent PL emission spectra of **(A)** 2.0 µL, **(B)** 4.0 µL, **(C)** 6.0 µL, **(D)** 8.0 µL and **(E)** 10.0 µL 0.1 mM of CuQ_2 (in ethanol) added Qdots dispersion (which contained 200.0 µL ethanolic solution of as synthesized Qdots and 2.8 mL ethanol). Data points were fitted to single exponential functions and the slopes were considered as initial rates of the reaction.

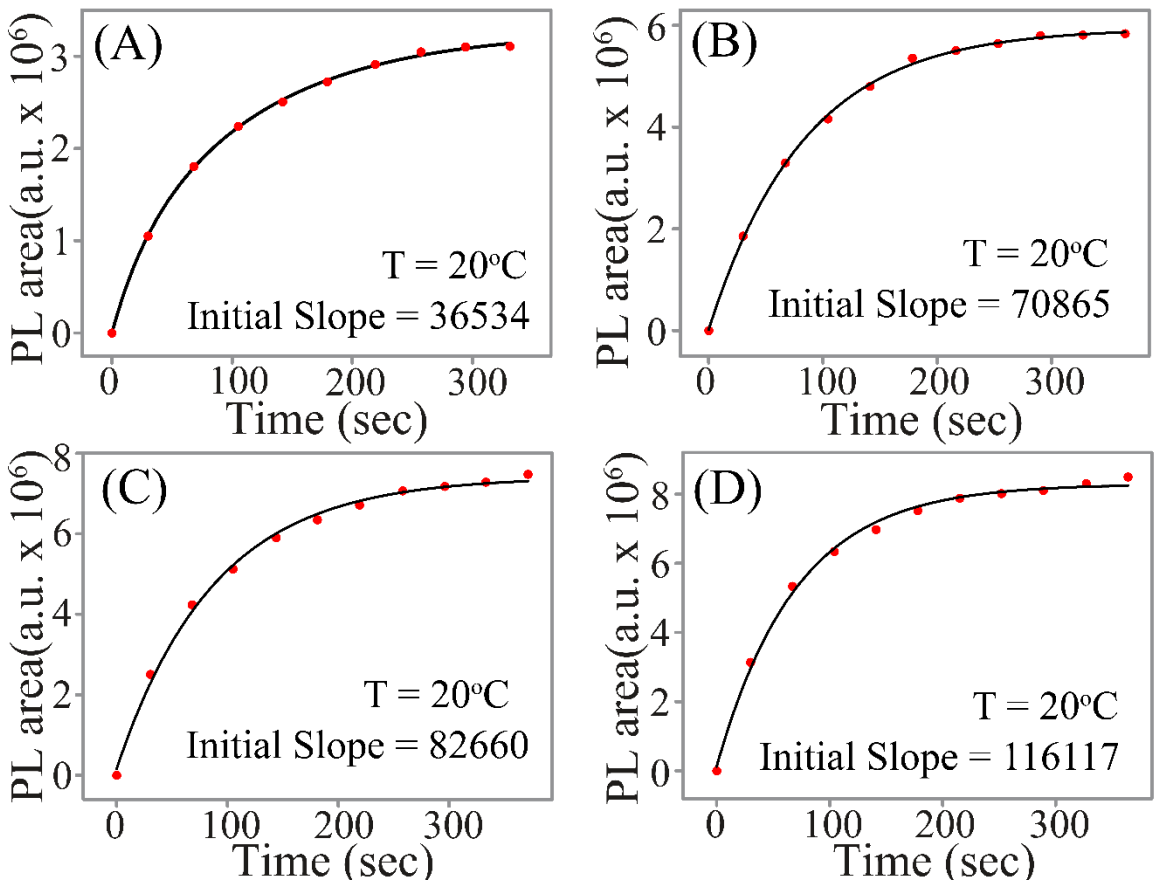

Figure S11. Exponential fittings of PL area (area under the emission curve) vs time plot at T= 20 °C obtained from time dependent PL emission spectra of **(A)** 2.0 μL, **(B)** 4.0 μL, **(C)** 6.0 μL and **(D)** 8.0 μL 0.1 mM of CuQ_2 (in ethanol) added Qdots dispersion (which contained 200.0 μL ethanolic solution of as synthesized Qdots and 2.8 mL ethanol). Data points were fitted to single exponential functions and the slopes were considered as initial rates of the reaction.

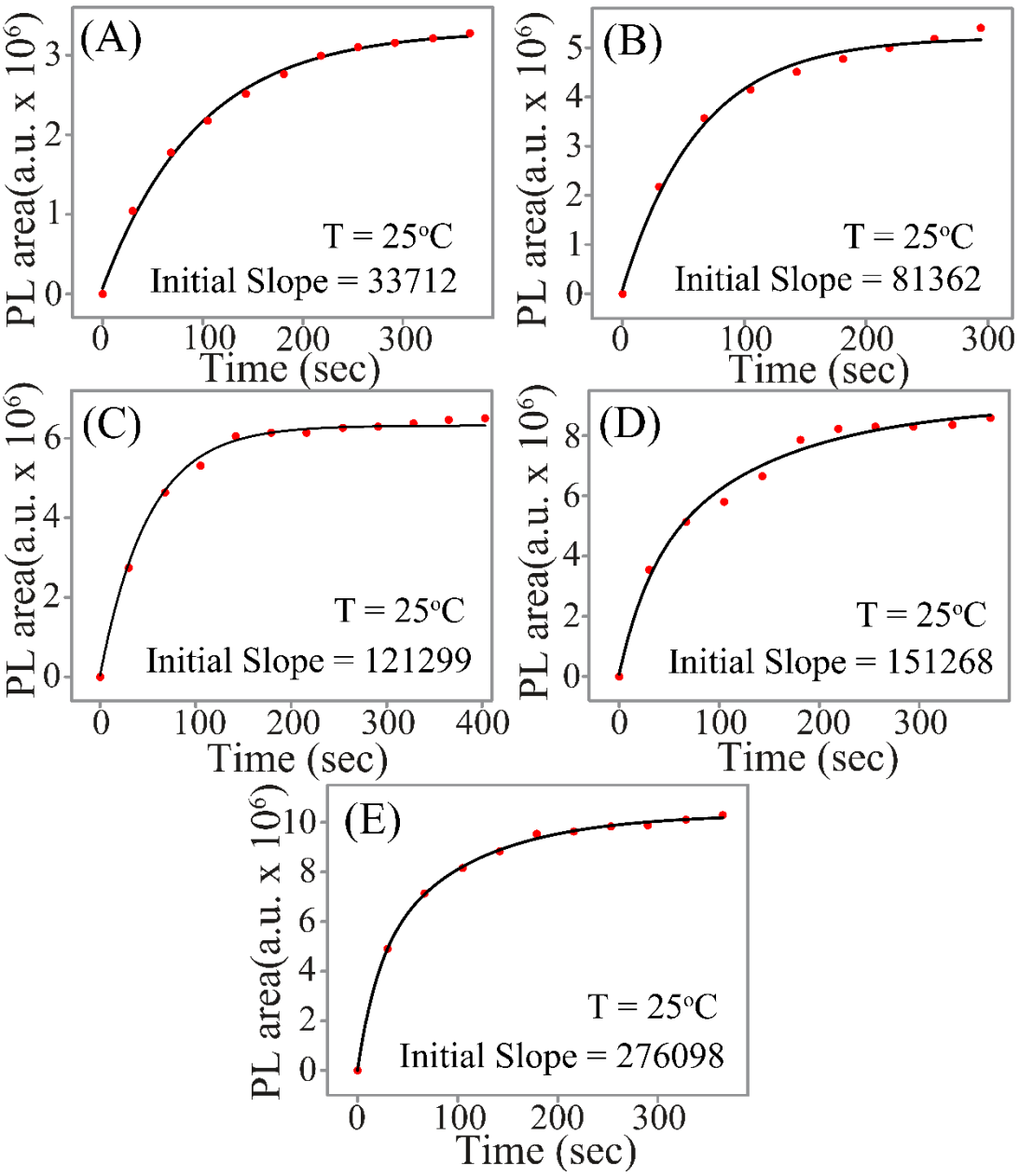

Figure S12. Exponential fittings of PL area (area under the emission curve) vs time plot at T= 25 ºC obtained from time dependent PL emission spectra of **(A)** 2.0 µL, **(B)** 4.0 µL, **(C)** 6.0 µL and **(D)** 8.0 µL, and **(E)** 10.0 µL 0.1 mM of CuQ_2 (in ethanol) added Qdot dispersion (which contained 200.0 µL ethanolic solution of as synthesized Qdots and 2.8 mL ethanol). Data points were fitted to single exponential functions and the slopes were considered as initial rates of the reaction.

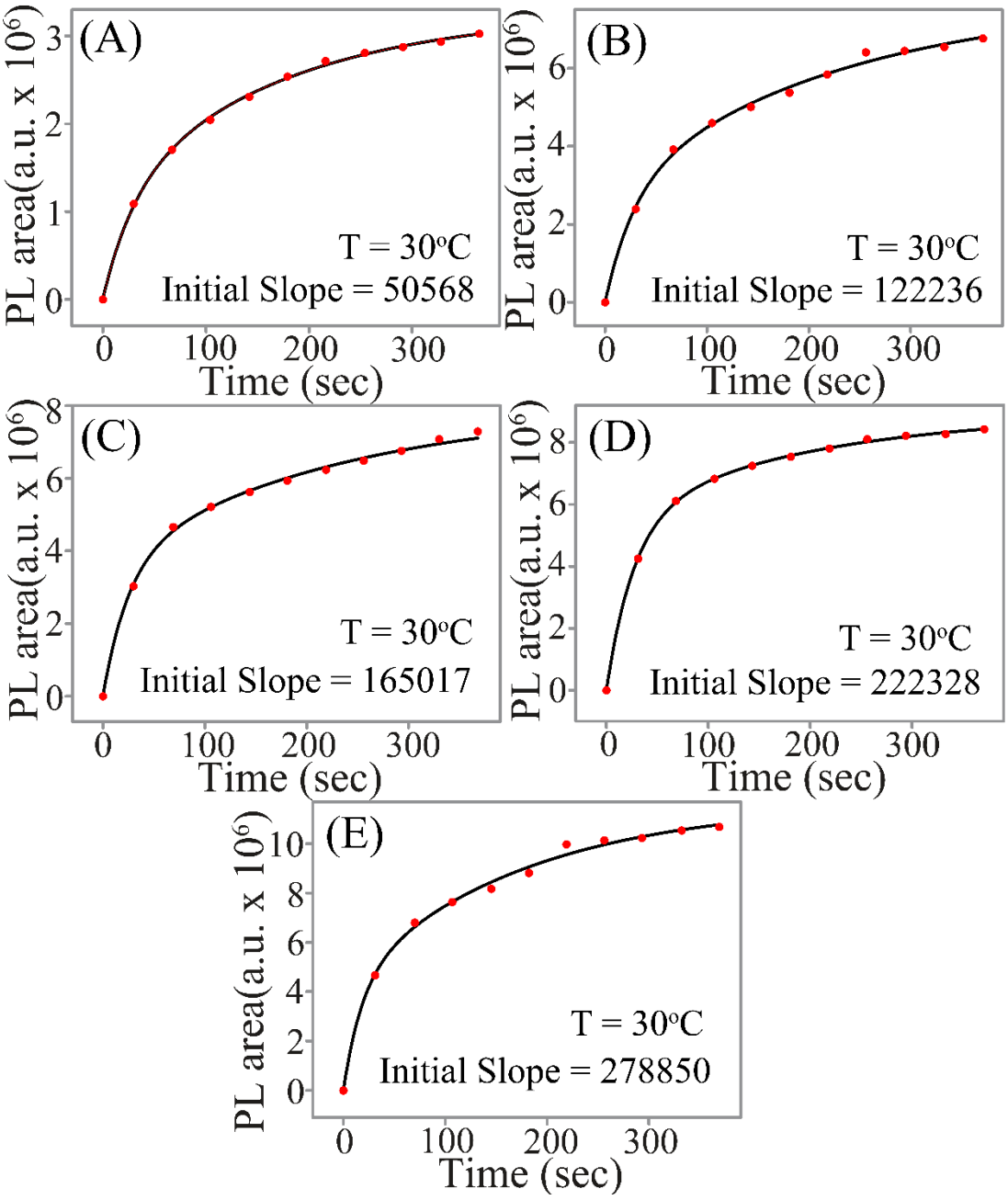

Figure S13. Exponential fittings of PL area (area under the emission curve) vs time plot at T= 30 ºC obtained from time dependent PL emission spectra of **(A)** 2.0 µL, **(B)** 4.0 µL, **(C)** 6.0 µL, **(D)** 8.0 µL and **(E)** 10.0 µL 0.1 mM of CuQ_2 (in ethanol) added Qdot dispersion (which contained 200.0 µL ethanolic solution of as synthesized Qdots and 2.8 mL ethanol). Data points were fitted to single exponential functions and the slopes were considered as initial rate of the reaction.

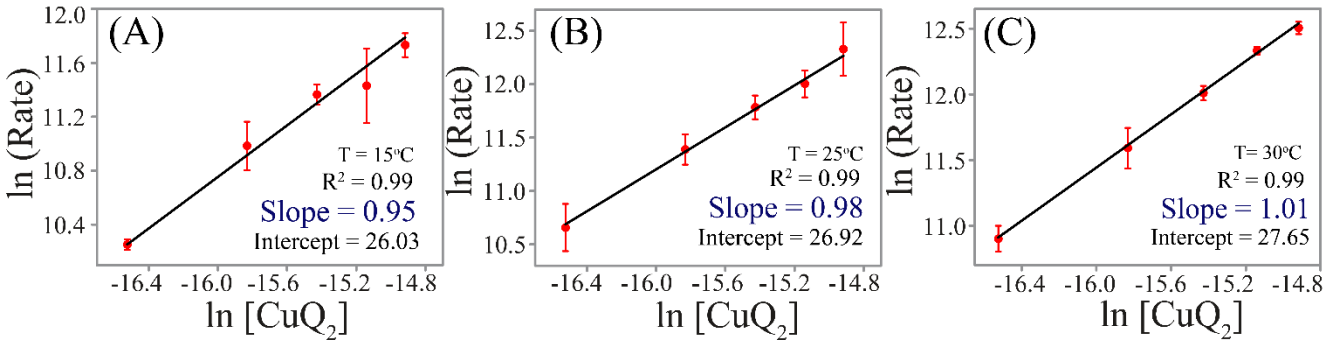

Figure S14. Plot of ln (Rate) Vs ln [CuQ_2] at different temperatures: **(A)** T= 15 ºC, **(B)** T= 25 °C and **(C)** T= 30 °C. Data points were fitted to linear functions and the slopes were considered equal to order of the reaction (i.e. 1).

Table S5: Tabulated form of the solutions, which were used for measuring order and activation energy of the formation of QDC with respect to CuQ_2.

Amount of 0.1 mM CuQ_2 used (µL)	Amount of as synthesized Qdots used (µL)	Amount of ethanol used (µL)	Total volume (µL)	Final concentration of CuQ_2 (µM)
2.0	200.0	2800.0	3002.0	0.07
4.0	200.0	2800.0	3004.0	0.13
6.0	200.0	2800.0	3006.0	0.20
8.0	200.0	2800.0	3008.0	0.26
10.0	200.0	2800.0	3010.0	0.33

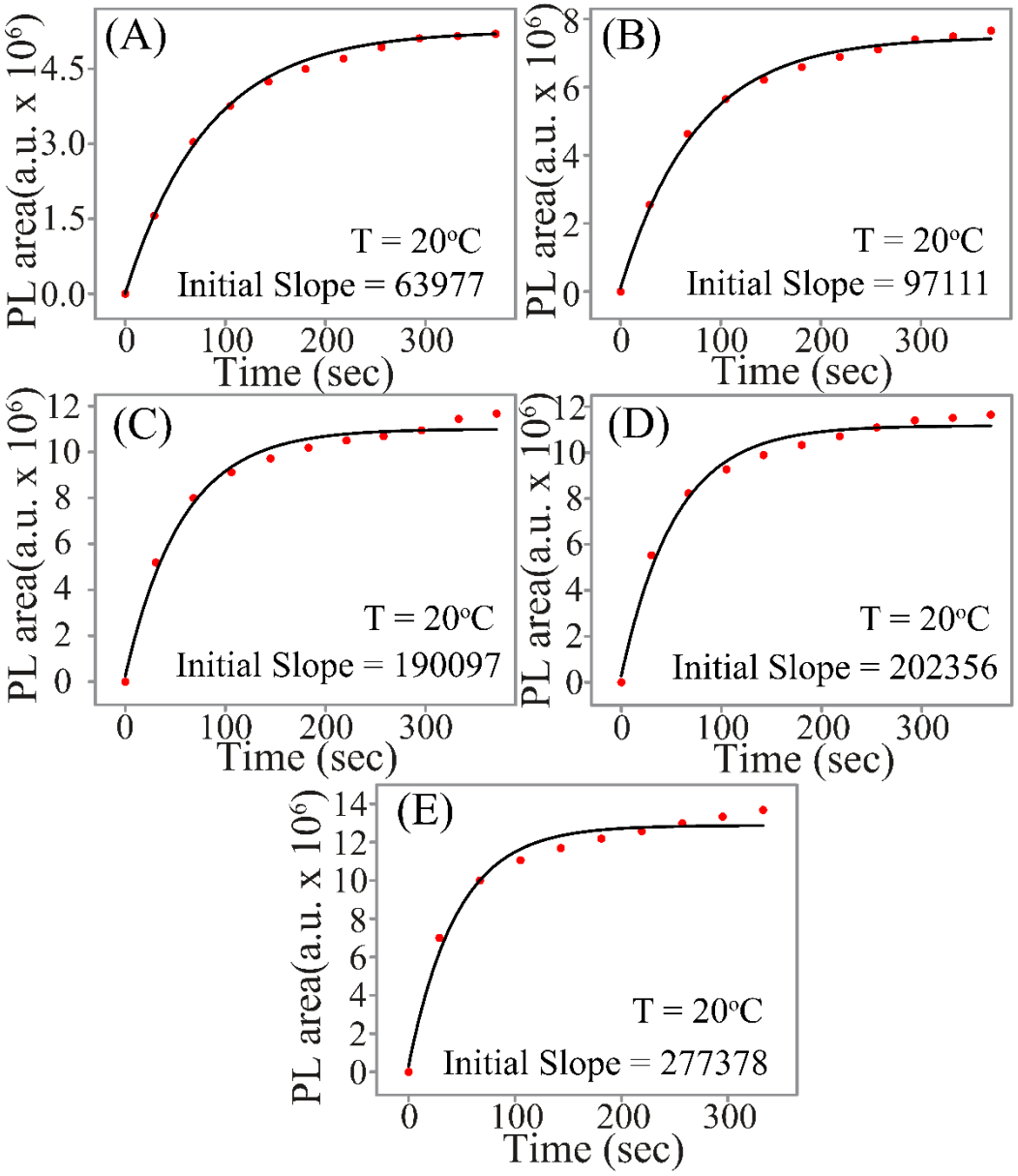

Figure S15. Exponential fittings of PL area (area under the emission curve) vs time plot at T= 20 °C obtained from time dependent PL emission spectra of 10.0 µL 0.1 mM of CuQ_2 (in ethanol) added to a solution which contained different volumes of as synthesized Qdots (in ethanol): **(A)** 50.0 µL, **(B)** 100.0 µL, **(C)** 150.0 µL, **(D)** 200.0 µL and **(E)** 250 µL Qdot dispersion. The total volume of each solution was adjusted to 3.0 mL by adding ethanol Data points were fitted to single exponential functions and the slopes were considered as initial rate of the reaction.

References:

1. Pan, H.; Liang, F.; Mao, C.; Zhu, J.; Chen, H. Highly Luminescent Zinc(II)-Bis(8-hydroxyquinoline) Complex Nanorods: Sonochemical Synthesis, Characterizations, and Protein Sensing. *J. Phys. Chem. B* **2007**, *111*, 5767- 5772.

2. Bhandari, S.; Roy, S.; Pramanik, S.; Chattopadhyay, A. Double Channel Emission from a Redox Active Single Component Quantum Dot Complex. *Langmuir* **2015**, *31*, 551- 561.

3. Bhandari, S.; Roy, S.; Chattopadhyay, A. Enhanced Photoluminescence and Thermal Stability of Zinc Quinolate Following Complexation on the Surface of Quantum Dot. *RSC Adv*. **2014**, *4*, 24217- 24221.

4. Crespi, M. S.; Ribeiro, C. A.; Greenhalf, V. C. M.; Zorel Jr, H. E. Preparation and Thermal Decomposition of Copper(II), Zinc(II) and Cadmium(II) Chelates with 8-Hydroxyquinoline. *Quím. Nova* **1999**, *22*, 41-46.

5. Acharya, S. A.; Maheshwari, N.; Tatikondewar, L.; Kshirsagar, A.; Kulkarni, S. K. Ethylenediamine-Mediated Wurtzite Phase Formation in ZnS. *Cryst. Growth Des*. **2013**, *13*, 1369- 1376.